Inorganic Chemistry

Article

pubs.acs.org/IC

From Stiba- and Bismaheteroboroxines to N,C,N-Chelated Diorganoantimony(III) and Bismuth(III) Cations—An Unexpected Case of Aryl Group Migration

Libor Dostál,*[,†] Roman Jambor,[†] Aleš Růžička,[†] Robert Jirásko,[‡] Antonín Lyčka,[§] Jens Beckmann,[∥] and Sergey Ketkov*[,⊥,#]

[†]Department of General and Inorganic Chemistry and [‡]Department of Analytical Chemistry, University of Pardubice, Studentská 573, CZ 532 10 Pardubice, Czech Republic

[§]Research Institute for Organic Syntheses, Rybitví 296, CZ 533 54 Pardubice, Czech Republic

[∥]Institut für Anorganische Chemie, Universität Bremen, Leobener Straße, 28359 Bremen, Germany

[⊥]G.A.Razuvaev Institute of Organometallic Chemistry, RAS, 49 Tropinin Street, 603950 Nizhny Novgorod, Russian Federation

[#]N.I. Lobachevsky Nizhny Novgorod State University, Gagarin Avenue 23, 603950 Nizhny Novgorod, Russian Federation

Supporting Information

ABSTRACT: An unprecedented transfer of an aryl group from boron to Sb and Bi is observed in the reaction of heteroboroxines of general formula ArM[$(OBR)_2O$] [where M = Sb, Bi; Ar = C_6H_3-2,6-$(CH_2NMe_2)_2$; R = Ph, 4-$CF_3C_6H_4$, 4-BrC_6H_4] with corresponding boronic acid $RB(OH)_2$. Using this procedure, ion pairs $[ArMR]^+[R_4B_5O_6]^-$ were obtained [where M = Sb and R = Ph (**4**), 4-$CF_3C_6H_4$ (**5**), 4-BrC_6H_4 (**6**); where M = Bi and R = Ph (**7**), 4-$CF_3C_6H_4$ (**8**), 4-BrC_6H_4 (**9**)]. All compounds were characterized using elemental analysis, electrospray ionization mass spectrometry, and multinuclear NMR spectroscopy, and molecular structures of **4** and **7** were determined by single-crystal X-ray diffraction analysis. The central metal atoms in **4**–**9** were arylated by respective boronic acids, which represents, to the best of our knowledge, unprecedented reaction path in the chemistry of heavier group 15 elements. Investigation of the mechanism of this transformation indicated that Lewis pairs consisting of monomeric oxides ArMO and boroxine rings are probably key intermediates. In this regard, molecular structures of $ArSbO[(4\text{-}CF_3C_6H_4)_3B_3O_3]\cdot(4\text{-}CF_3C_6H_4)B(OH)_2$ (**10**) and $\{ArSbO[(3,5\text{-}(CF_3)_2C_6H_3)_3B_3O_3]\}$ (**13**) were established by single-crystal X-ray diffraction analysis, and compound **13** was also fully characterized in solution by multinuclear NMR spectroscopy. The bonding in **13** was analyzed in detail by using density functional theory and natural bond order calculations and compared with known adduct $ArSbOB(C_6F_5)_3$ (**14**) and hypothetical ArSbO monomer.

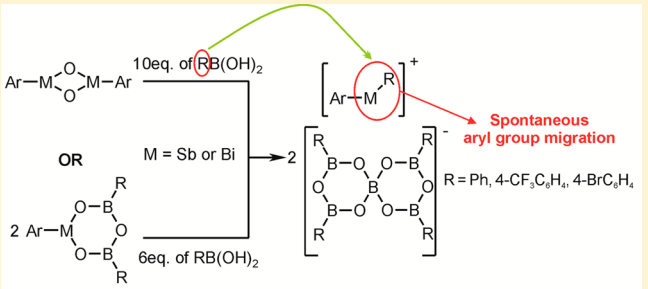

INTRODUCTION

The chemistry of molecular boroxines, which can be regarded as anhydrides of boronic acids, represents a rather rich and miscellaneous branch of main-group element chemistry that is still intensively developed leading to widespread applications in both synthetic and material science.[1] From this viewpoint, molecular heteroboroxines, that is, compounds containing a heteroatom instead of boron in the central inorganic core, seem to constitute an attractive class of inorganic ring systems (Figure 1).[1b]

Such heteroboroxines have been known for years, but their chemistry is still quite unexplored. The structurally authenticated molecular heteroboroxines with the central MB_2O_3 core include those derived from Al, Si, P, and Sn.[2] There are also a limited number of molecular compounds with eight-membered rings of the type $Si_2B_2O_4$.[3] We recently entered this field demonstrating that series of stiba-, bisma-, and stannaboroxines

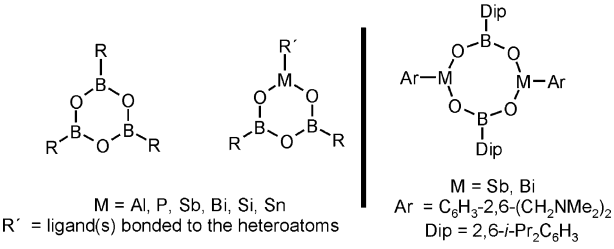

Figure 1. General structures of boroxines and selected heteroboroxines containing both six- and eight-membered rings.

with central six-membered MB_2O_3 core (where M = Sb, Bi, or Sn) are quite easily accessible via simple condensation reaction

Received: April 20, 2015
Published: May 27, 2015

DOI: 10.1021/acs.inorgchem.5b00893
Inorg. Chem. 2015, 54, 6010–6019

of parent boronic acids and proper organometallic precursors, namely, oxides $(ArSbO)_2$ (**1**) and $(ArBiO)_2$ (**2**) or organotin(IV) carbonate $Ar(Ph)Sn(CO_3)$ (**3**) [where Ar is an abbreviation for the N,C,N-chelating ligand C_6H_3-2,6-$(CH_2NMe_2)_2$].[4] It has also been shown that analogous heteroboroxines could be obtained by a conversion between boroxine rings $R_3B_3O_3$ (R = Me or MeO) and **1**−**3**.[5] Finally, we also demonstrated that eight-membered stiba- and bismaboroxines containing central $M_2B_2O_4$ rings (where M = Sb or Bi, Figure 1) can be isolated provided the bulky 2,6-*i*-$Pr_2C_6H_3$ (Dip) substituent is attached to the boron atom.[6] These results indicate that the stoichiometry is crucial for the outcome of the condensation reaction of **1**−**3** with boronic acids.

Herein, we report on reactions of $(ArSbO)_2$ (**1**) and $(ArBiO)_2$ (**2**) with an excess (10 mol equiv) of selected boronic acids $RB(OH)_2$ (where R = Ph, 4-$CF_3C_6H_4$, 4-BrC_6H_4), which surprisingly resulted in an arylation of the antimony or bismuth atom by respective boronic acid. The plausible mechanism of these reactions was suggested as well.

RESULTS AND DISCUSSION

While the reaction of oxides $(ArSbO)_2$ (**1**)[7] and $(ArBiO)_2$ (**2**)[8] with four molar equivalents of respective boronic acids resulted in the formation of six-membered heteroboroxine rings (Scheme 1A[4a,b]), the changing of the stoichiometry to 1:10

Scheme 1. Preparation of 4−9

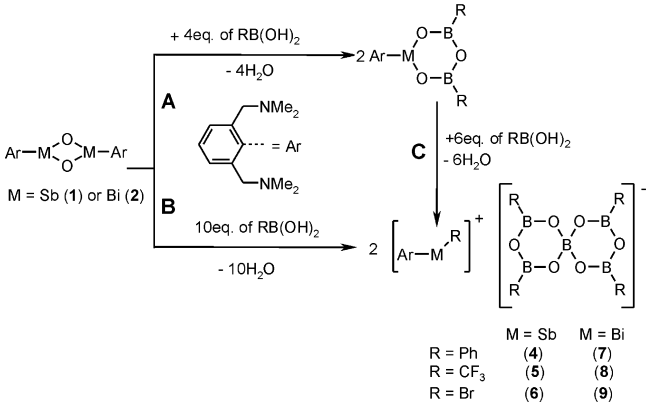

led to the formation of $[ArMR]^+[R_4B_5O_6]^-$ [where M = Sb and R = Ph (**4**), 4-$CF_3C_6H_4$ (**5**), 4-BrC_6H_4 (**6**); where M = Bi and R = Ph (**7**), 4-$CF_3C_6H_4$ (**8**), 4-BrC_6H_4 (**9**)] (Scheme 1B). Importantly, **4**−**9** are also easily (and more conveniently) accessible by the conversion of respective heteroboroxines $ArM[(OBR)_2O]$ with 3 mol equiv (*per* one heteroboroxine) of boronic acid (Scheme 1C) suggesting that these heteroboroxines themselves play an important role in the formation of final products **4**−**9** (see further Discussion Section). Compounds **4**−**9** were isolated as colorless crystalline solids in reasonable yields (54−71%, Scheme 1C), which are well-soluble in chlorinated solvents but nearly insoluble in aliphatic solvents. Compounds **4**−**9** form ion pairs consisting of nonsymmetrically substituted $[ArMR]^+$ cations and *spiro*-borate $[R_4B_5O_6]^-$ counteranions. The identity of **4**− **9** was established by elemental analysis and electrospray ionization (ESI) mass spectrometry (MS). Because of the ionic behavior of **4**−**9**, all studied compounds provide characteristic mass spectra[9] yielding two complementary ions with expected *m*/*z* values (see the Experimental Section), that is, $[ArMR]^+$ cations in the positive mode and corresponding $[R_4B_5O_6]^-$ anions in the negative mode. In solution, the structure of **4**−**9** was proven by ^1H, ^{13}C, ^{11}B, and ^{19}F (for **5** and **8**) NMR spectroscopy. The ^1H NMR spectra of **4**−**9** in $CDCl_3$ at 295 K revealed a sharp AB pattern for CH_2N groups and two sharp singlets for magnetically nonequivalent $(CH_3)_2N$ moieties, thereby proving the presence of nonsymmetrically substituted diorganoantimony(bismuth) cations. One set of signals for the metal (Sb or Bi) bonded aryl group was detected in ^1H and ^{13}C spectra (see the Experimental Section). Furthermore, one set of signals was also observed for aryl substituents bonded to the boron atoms in spiro anions. In the case of **5** and **8**, two signals were detected in corresponding ^{19}F NMR spectra (in mutual 1:4 integral ratio), which is consistent with the presence of both $[ArM(4\text{-}CF_3C_6H_4)]^+$ cation and corresponding $[(4\text{-}CF_3C_6H_4)_4B_5O_6]^-$ anion (at −62.5 and −63.4 ppm for **5**, at −62.6 and −63.3 ppm for **8**). Finally, ^{11}B NMR spectra contained two signals in each case. One of them observed in the range of 27.8−29.8 ppm indicates the presence of boroxine-like boron atom, while the second one falls within the region (0.20−0.46 ppm) typical for boron atoms located in the spiro-BO_4^- environment.[10]

Molecular structures of $[ArSbPh]^+[Ph_4B_5O_6]^-$ (**4**) and $[ArBiPh]^+[Ph_4B_5O_6]^-$ (crystallized as a solvate $7{\cdot}H_2O$) were unambiguously established by means of single-crystal X-ray diffraction analysis and are shown in Figures 2 and 3 together

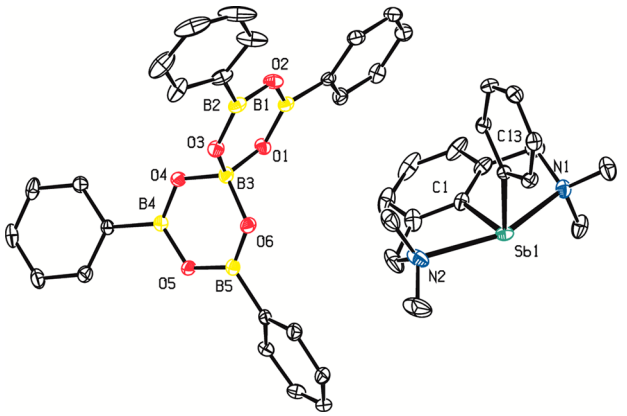

Figure 2. ORTEP plot of molecule of **4**. Hydrogen atoms were omitted for clarity. Anisotropic displacement parameters are depicted at the 40% probability level. Selected bond lengths (Å) and angles (deg): Sb(1)−N(1) 2.385(3), Sb(1)−N(2) 2.423(3), Sb(1)−C(1) 2.102(3), Sb(1)−C(13) 2.136(3), B(3)−O(1) 1.474(4), B(3)−O(3) 1.469(4), B(3)−O(4) 1.471(4), B(3)−O(6) 1.477(4), B(1)−O(1) 1.338(4), B(1)−O(2) 1.388(4), B(2)−O(2) 1.393(4), B(2)−O(3) 1.330(4), B(4)−O(4) 1.336(4), B(4)−O(5) 1.390(4), B(5)−O(5) 1.384(4), B(5)−O(6) 1.340(4), N(1)−Sb(1)−N(2) 148.90(9).

with selected structural parameters. Both structures consist of well-separated ion pairs $[ArMPh]^+[Ph_4B_5O_6]^-$ (where M = Sb for **4** and Bi for **7**) as there is no significant contact between central atoms (Sb or Bi) and corresponding spiro-borate anion. The pnictogen atom of the cation is coordinated by the NCN donor set of the ligand [N-M-N bonding angles amount to 148.90(9)° in **4** and 145.1(2)° in **7**]. The intramolecular N → M interactions are characterized by respective distances [Sb(1)−N(1) 2.385(3) Å and Sb(1)−N(2) 2.423(3) Å in **4**, Bi(1)−N(1) 2.520(7)Å and Bi(1)−N(2) 2.509(6) Å in **7**, $\sum_{cov}$(M, N) = 2.11 (Sb) and 2.22 Å (Bi)[11]]. These values are comparable to those found in related N,C,N-chelated antimony

DOI: 10.1021/acs.inorgchem.5b00893
Inorg. Chem. 2015, 54, 6010−6019

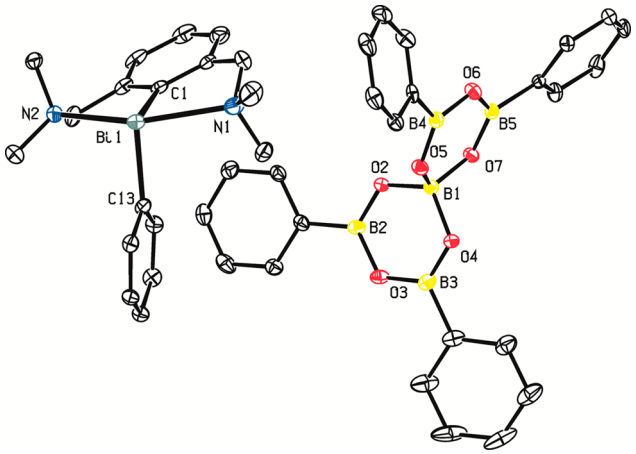

Figure 3. ORTEP plot of molecule of $7{\cdot}H_2O$. Hydrogen atoms and water molecule were omitted for clarity. Anisotropic displacement parameters are depicted at the 40% probability level. Symmetry operator: $a = 1/2 + x, 3/2 - y, 2 - z$. Selected bond lengths (Å) and angles (deg): Bi(1)–N(1) 2.520(7), Bi(1)–N(2) 2.509(6), Bi(1)–C(1) 2.202(6), Bi(1)–C(13) 2.235(7), B(1)–O(2) 1.474(9), B(1)–O(4) 1.469(9), B(1)–O(5) 1.471(10), B(1)–O(7) 1.470(9), B(2)–O(2) 1.344(9), B(2)–O(3) 1.393(9), B(3)–O(3) 1.383(9), B(3)–O(4) 1.335(10), B(4)–O(5) 1.344(8), B(4)–O(6) 1.378(9), B(5)–O(6) 1.383(8), B(5)–O(7) 1.341(8), N(1)–Bi(1)–N(2) 145.1(2).

and bismuth cations such as $\{[C_6H_3\text{-}2,6\text{-}(CH_2NMe_2)_2]\text{-}SbCl\}^+[CB_{11}H_{12}]^-$ [Sb–N distances: 2.379(5) and 2.422(4) Å[12]], $\{[C_6H_3\text{-}2,6\text{-}(CH_2NMe_2)_2]_2Bi\}^+[BPh_4]^-$ [Bi–N-(coordinated) distances: 2.509(2) and 2.552(2) Å[13]] or $\{[C_6H_3\text{-}2\text{-}(CH_2NMe_2)_2\text{-}6\text{-}(CH_2O\text{-}t\text{-}Bu)]BiCl\}^+[CB_{11}H_{12}]^-$ [Bi–N distance: 2.420(5) Å[14]]. The spatial arrangement is best described as a vacant ψ-square pyramid, with nitrogen and carbon atoms forming a strongly distorted basal plane [as demonstrated especially by the bonding angles C(ipso)-Sb(Bi)-N in the range of 72.4(2)–74.50(11)° being far from the ideal value 90°] and the lone pair of the respective central atom located in apical position.

The spiro-counteranion $[Ph_4B_5O_6]^-$ in **4** and **7** is built from two six-membered B_3O_3 rings sharing one boron atom. The four B(spiro)–O bond lengths [in the range of 1.469(4)–1.477(4) Å] are significantly elongated in comparison with the remaining B–O bonds [in the range of 1.330(4)–1.393(10) Å] in these anions, but all B–O bonds are still slightly shorter than would be expected for B–O single bonds [$\sum_{cov}$(B, O) = 1.48 Å[11]]. The overall structure of $[Ph_4B_5O_6]^-$ is, thus, analogous to that described for the same $[Ph_4B_5O_6]^-$ anion before by Johnson et al.[15]

Proposed Mechanism. In the course of our initial investigation dealing with ideal stoichiometry for the formation of compounds **4**–**9** made by NMR spectroscopy, we noticed the formation of an intermediate containing the ligand Ar, which is during the course of reaction converted to the final products **4**–**9** (for example see the formation of **5** as monitored by ^{1}H NMR spectroscopy in the Supporting Information, Figure S1). We serendipitously obtained a small amount of single crystals in the sample made from the heteroboroxine $ArSb[(OBR)_2O]$ and corresponding boronic acid $RB(OH)_2$ (R = 4-$CF_3C_6H_4$), and the molecular structure was determined using single-crystal X-ray diffraction analysis (Scheme 2 and Figure 4). The observed structure of $ArSbO[(4\text{-}CF_3C_6H_4)_3B_3O_3]\cdot(4\text{-}CF_3C_6H_4)B(OH)_2$ (**10**) is unprecedented.

Scheme 2. Proposed Formation of 10

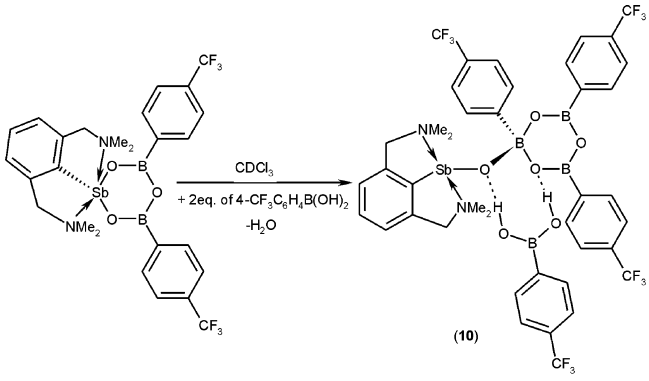

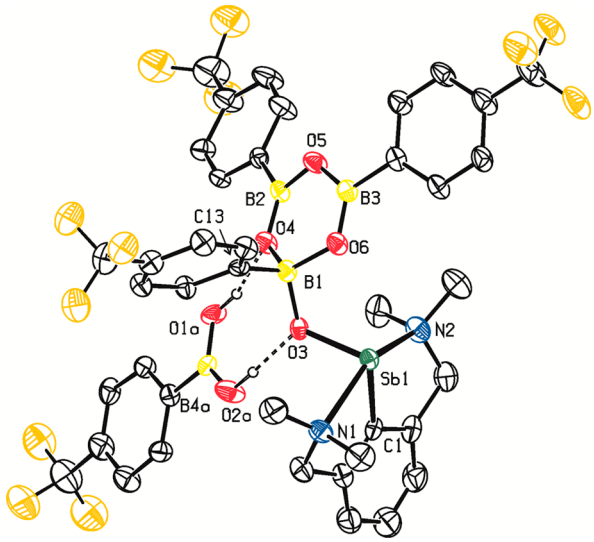

Figure 4. ORTEP plot of molecule of **10**. Hydrogen atoms (except those of boronic acid) were omitted for clarity. Only one position of disordered fluorine atoms in the CF_3 groups is shown. Anisotropic displacement parameters are depicted at the 30% probability level. The symmetry operator $a = 1 - x, 1 - y, -z$. Selected bond lengths (Å) and angles (deg): Sb(1)–N(1) 2.412(14), Sb(1)–N(2) 2.447(14), Sb(1)–C(1) 2.117(16), Sb(1)–O(3) 1.954(10), B(1)–O(3) 1.48(2), B(1)–O(4) 1.530(16), B(1)–O(6) 1.47(2), O(1a)–O(4) 2.830(17), O(2a)–O(3) 2.731(17), N(1)–Sb(1)–N(2) 148.1(5), C(1)–Sb(1)–O(3) 99.6(5), Sb(1)–O(3)–B(1) 117.2(9), O(1a)–H(O1a)–O(4) 166, O(2a)–H(O2a)–O(3) 169.

It consists of central boroxine core, which is connected via O(3) → B(1) contact [1.48(2) Å] to the molecule of the antimony oxide; that is, the antimony oxide is eliminated from the original heteroboroxine ring and replaced by the boronic acid. The spatial arrangement of the B(3) atom is due to this interaction tetrahedral and the aryl group seems to be in promising environment for its migration to the antimony atom. In addition, there is another molecule of boronic acid, which is tightly attached to the central core through two hydrogen bonds [O(1a)–O(4) 2.830(17) and O(2a)–O(3) 2.731(17) Å]. Importantly, these contacts are directed to the oxygen atoms O(3) and O(4) both of them laying in the vicinity of the crucial O(3) → B(1) contact. Finally, this interaction proves the possibility for additional boronic acids to enter the boroxine core that may lead to the formation of spiro-counteranion (via dehydration) after migration of the organic group to the antimony atom. All our numerous attempts to isolated similar

DOI: 10.1021/acs.inorgchem.5b00893
Inorg. Chem. 2015, 54, 6010–6019

intermediates using boronic acids $RB(OH)_2$ (where R = Ph, 4-$CF_3C_6H_4$, 4−Br-C_6H_4) involved in final products **4**−**9** on a preparative scale failed.

Structure of **10** may be viewed as a Lewis pair formed between electron-rich terminal oxygen atom in formally monomeric oxide ArSbO with polarized Sb^+-O^- bond and a boron atom from the boroxine core as an electron acceptor (see further Discussion Section below). We note a large number of 1:1 adducts of six-membered boroxine rings $R_3B_3O_3$·LB with Lewis bases (LB) including amines, N-heterocyclic carbenes (NHCs).[16] Boron atoms in boroxines are inherently Lewis acidic, but only of one of boron atoms is usually involved in an interaction with an LB. In addition, the phenomenon of stabilization of formally double M=O bonds by their interaction with Lewis acids and(or) bases has been recently recognized and utilized, for example, in stabilization of previously elusive terminal M═O bonds (M = Si, Ge) as well.[17]

This formalism led to the idea that increasing of the Lewis acidity of boron atoms within the boroxine core should significantly support the stability ArSbO(boroxine) adducts. Heteroboroxines **11** and **12** substituted by electron-withdrawing 3,5-$(CF_3)_2C_6H_4$ groups were prepared for this purpose (Scheme 3). They were isolated in good yields (75 and 64%,

Scheme 3. Preparation of 11−13

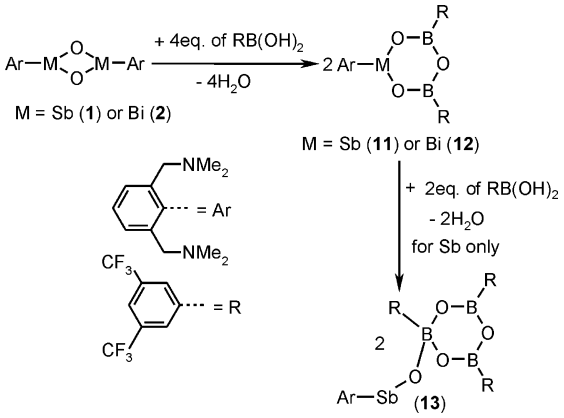

respectively) as colorless crystalline solids well-soluble in chlorinated solvents. The ^{1}H NMR spectra of **11** and **12** in $CDCl_3$ at 295 K revealed a sharp AB pattern for CH_2N and two singlets for magnetically nonequivalent $(CH_3)_2N$ moieties and one set of signals for 3,5-$(CF_3)_2C_6H_4$ groups in expected mutual integral ratio. Similarly, one set of appropriate signals was observed in corresponding ^{13}C NMR spectra of **11** and **12**. ^{19}F and ^{11}B NMR spectra showed one signal at −62.9 and 27.3 ppm (26.8 ppm for **12**), respectively. The molecular structure of **11** was unambiguously established using single-crystal X-ray diffraction analysis (Figure 5).

Compound **11** exhibits structural features typical for other structurally authenticated stibaboroxines[4] (thus is not discussed here in more detail). The central SbB_2O_3 ring is nearly planar, and the flanking boron-bonded aryl groups remain coplanar with this central core. In contrast, the pincer ligand is nearly perpendicular to the mean SbB_2O_3 plane. The Sb(1) atom is effectively stabilized by coordination of the NCN donor set (for relevant structural parameters, see Figure 5).

Compound **11** smoothly reacts with one molar equivalent of parent boronic acid under formation of **13**, which was isolated in very high yield (the NMR investigation suggests a

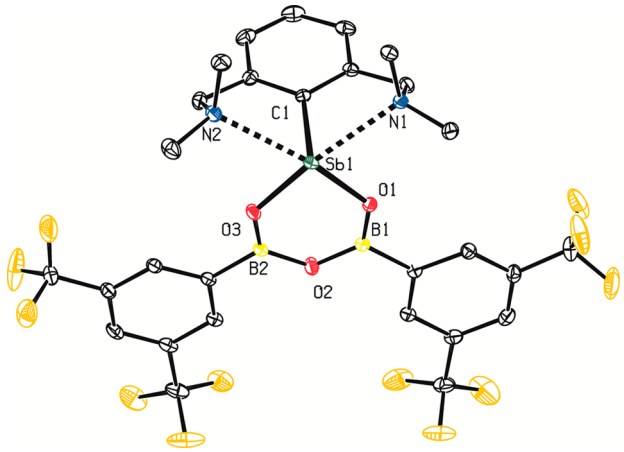

Figure 5. ORTEP plot of molecule of **11**. Hydrogen atoms were omitted for clarity. Anisotropic displacement parameters are depicted at the 40% probability level. Selected bond lengths (Å) and angles (deg): Sb(1)−N(1) 2.601(2), Sb(1)−N(2) 2.632(3), Sb(1)−C(1) 2.144(2), Sb(1)−O(1) 2.057(2), Sb(1)−O(3) 2.0530(18), B(1)−O(1) 1.331(3), B(1)−O(2) 1.387(3), B(2)−O(2) 1.381(4), B(2)−O(3) 1.329(3), N(1)−Sb(1)−N(2) 118.57(7), O(1)−Sb(1)−O(3) 85.94(8), N(1)−Sb(1)−O(1) 74.17(7), N(2)−Sb(1)−O(3) 73.13(8).

quantitative conversion) as colorless crystalline solid well-soluble in chlorinated solvents. The ^{1}H NMR spectrum of **13** contains an AB system for CH_2N and two sharp singlets for magnetically nonequivalent $(CH_3)_2N$ moieties. Two sets of signals for nonequivalent 3,5-$(CF_3)_2C_6H_4$ groups were detected in corresponding ^{1}H and ^{13}C NMR spectra. Similarly, two signals in mutual 1:2 integral ratio were observed in corresponding ^{19}F NMR spectrum consistently with the proposed structure of **13**. Finally, the ^{11}B NMR spectrum revealed two signals at 27.9 ppm for classical boroxine-like boron atom and at 3.0 ppm for a tetrahedraly coordinated boron atom.[10] It is important to note that compound **13** does not react with additional boronic acid under the same conditions as used for preparation of **4**−**9**, thereby proving the exceptional stability of the adduct **13**. Molecular structure of **13** was confirmed by single-crystal X-ray diffraction analysis and resembles the structure of **10** (Figures 6 and 7).

Accordingly, the antimony oxide was formally eliminated from the stibaboroxine core of starting **11** and is connected to newly formed boroxine-core via tight O(1) → B(1) contact [1.456(4) Å] (for more detailed discussion of the bonding situation, see further Discussion). The spatial arrangement of the B(1) atom is tetrahedral and similar to that of B(3) atom in **10**.

Smooth formation of **13** in the reaction between **11** and the boronic acid strongly supports our previous consideration about proposed reaction mechanism (including the structure of **10**) explaining formation of **4**−**9** that is summarized in Scheme 4. Thus, classical heteroboroxine is formed in the first step of this procedure followed by the reaction with another equivalent of boronic acid leading to the formation of more or less stable Lewis adduct between the boroxine and oxide **1** or **2**. The tetrahedral boron atom involved in these adducts seems to play a crucial role in the arylation of the antimony (or bismuth) atom, which is then followed by the reaction with two more equivalents of boronic acid and formation of final spiro counteranion and organoantimony or organobismuth cation. It is important to note that we failed in the isolation of an analogue of **13** (Figure 6) in the case of bismuth, but this may

DOI: 10.1021/acs.inorgchem.5b00893
Inorg. Chem. 2015, 54, 6010−6019

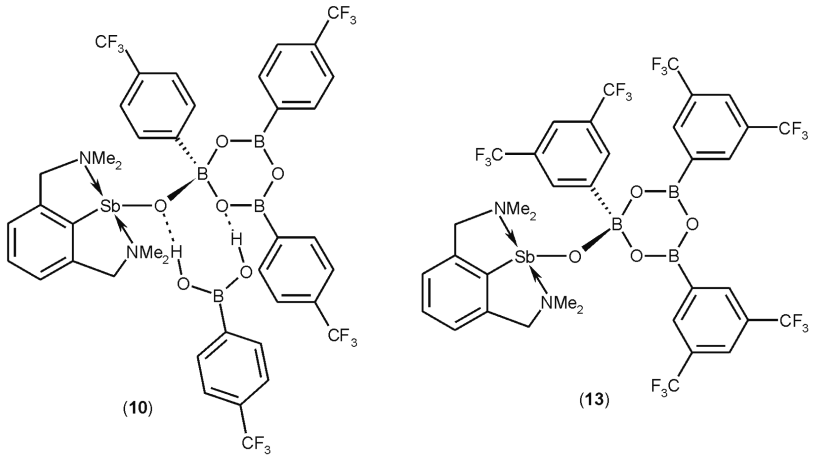

Figure 6. Presentation of structures as determined by X-ray diffraction analysis of **10** (left, showing also via hydrogen bonds attached boronic acid) and **13** (right).

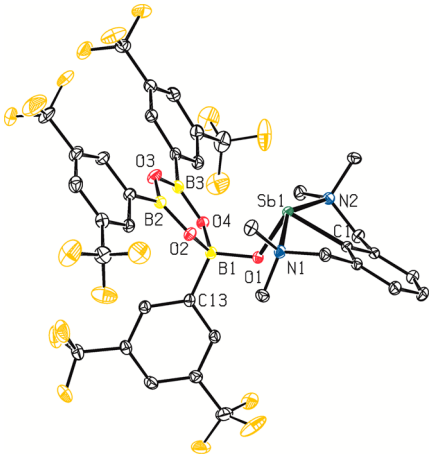

Figure 7. ORTEP plot of molecule of **13**. Hydrogen atoms were omitted for clarity. Anisotropic displacement parameters are depicted at the 40% probability level. Selected bond lengths (Å) and angles (deg): Sb(1)−N(1) 2.414(3), Sb(1)−N(2) 2.400(3), Sb(1)−C(1) 2.111(3), Sb(1)−O(1) 1.925(3), B(1)−O(1) 1.456(4), B(1)−O(2) 1.503(5), B(1)−O(4) 1.492(5), B(1)−C(13) 1.622(6), B(2)−O(2) 1.340(5), B(2)−O(3) 1.379(5), B(3)−O(3) 1.385(6), B(3)−O(4) 1.339(5), N(1)−Sb(1)−N(2) 148.85(10), C(1)−Sb(1)−O(1) 95.56(14), Sb(1)−O(1)−B(1) 118.0(2).

Scheme 4. Schematic Presentation of Plausible Mechanism for Arylation of Antimony or Bismuth Atoms in the Reaction between 1 or 2 and Corresponding Boronic Acid

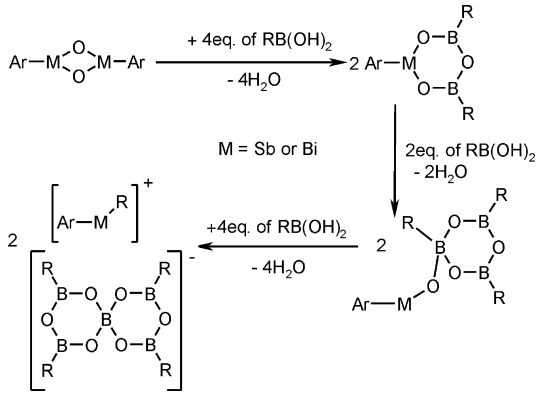

be mainly ascribed to expected lower stability of such an adduct (noteworthy, heteroboroxine **12** itself exhibits only limited stability and decomposes in a period of several days in solution).

Theoretical Analysis of the Bonding in 13. The formation of **10** and **13** deserves further comment. We recently succeeded in the isolation of a full series of terminal Sb−E bonds (E = S, Se, Te) using thermodynamic stabilization of these bonds by N,C,N pincer-type ligands, although these bonds are significantly polarized [$^{+}$Sb−E^{-}] as demonstrated by both experimental and theoretical studies.[18] The positive charge on the central antimony atom is compensated by the electron density coming from the nitrogen donor atoms.[18] In contrast, both N,C,N-chelated antimony and bismuth oxides prefer dimeric structures with bridging oxygen atoms.[7,8] Only recently, we succeeded in the isolation of the first monomeric antimony oxide ArSbOB(C_6F_5)$_3$ (**14**) as the adduct with Lewis acid.[19] Compound **13**, thus, represents another example of monomeric organoantimony(III) oxide with a formally terminal Sb═O bonds trapped in the coordination sphere of a Lewis acid. The Sb(1)−O(1) bond 1.925(3) Å in **13** is significantly shorter than those in starting oxide **1** [2.000(3) and 2.018(3) Å] and is comparable to the value found in **14** [1.923(2) Å], but it is significantly shorter than $\sum_{cov}$(Sb,O) = 2.14 Å.[11] More importantly, these Sb−O distances approach the theoretical value for Sb═O double bond 1.90 Å.[11] Similarly, B(1)−O(1) distance [1.456(4) Å] well coincides with that previously reported for **14** [1.470(3) Å] and are slightly shorter than $\sum_{cov}$(B, O) = 1.48 Å.[11]

To get more detailed information on the nature of electronic interactions in the ArSbO(boroxine) systems, we performed density functional theory (DFT) calculations of **13** at the M062X/DGDZVP level of theory and compared the results with the computational data obtained for **14**[19] and elusive ArSb═O. The optimized geometries of **13** and **14** reproduce correctly the experimental Sb−O and B−O bond lengths (Supporting Information, Table S1). The calculated Sb−O−B angle increases from 118.0° to 135.0° on going from **13** to **14**, which correlates very well with the X-ray diffraction results [118.0° (Figure 7) and 134.0°,[19] respectively). This increase arises from the steric repulsion between the L fragment and C_6F_5 groups in **14**. As a result, the positive deformation electron density (DED) corresponding to the Sb−O and B−O

DOI: 10.1021/acs.inorgchem.5b00893
Inorg. Chem. 2015, 54, 6010−6019

bonds in **13** is higher than that in **14** (Figure 8). In the latter molecule, the larger Sb−O−B angle leads to a shift of the DED

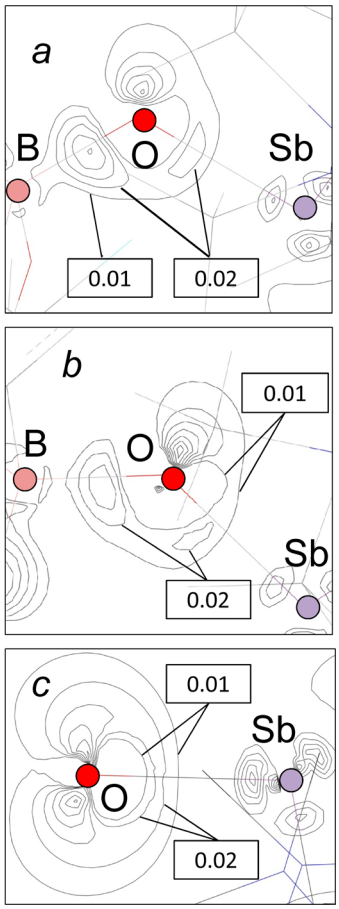

Figure 8. Calculated contours (0.01−0.1 au, step 0.01 a.u) of the positive deformation electron density in the SbOB plane of **13** (a) and **14** (b) and in the SbOC plane of ArSbO (c).

maxima from the lines connecting the atomic nuclei (Figure 8b). These changes should weaken the Sb−O and B−O covalent interactions in **14** as compared to **13**. Accordingly, the electron density in the B−O bonding critical point (BCP) decreases from 0.157 au in **13** to 0.147 au in **14** (Table S1). The ratio of the local potential-energy density and local kinetic-energy density $|V|/G$ at the Sb−O and B−O BCPs decreases on going from **13** to **14** (Table S1), which is indicative of the higher ionic contribution to the corresponding bonds in **14**.[20]

However, the B1 positive charge in **13** is larger than that in **14**, while the O and Sb charges are similar (Supporting Information, Table S2). The B−O ionic interaction in **14** is, therefore, weaker than in **13**, and one can conclude that the B−O dissociation energy should be higher for the complex with the boroxine fragment. Such a conclusion is supported by the energy decomposition analysis (EDA),[21] which reveals higher energy of the repulsive steric interactions in **14** and, as a consequence, less energetically favorable total interaction between the organoboron and organoantimony fragments in $ArSbOB(C_6F_5)_3$ (**14**) (Supporting Information, Table S3).[19] However, surprisingly, the calculations of the B−O dissociation energies on the basis of the energies of optimized fragments with the basis set superposition error (BSSE) correction give 55.7 and 64.4 kcal mol^{-1} for **13** and **14**, respectively. This contradiction is a result of the higher reorganization energy of boroxine upon formation of the **13** as compared to that of $ArSbOB(C_6F_5)_3$ (**14**). Despite the higher dissociation energy, the **14** molecule should be less kinetically stable than complex **13** because of the weaker B−O interaction in **14**. The NBO analysis[22] reveals different frontier Lewis pair structures describing **13**, **14**, and ArSbO. According to the NBO approach, the Sb atom of the latter possesses one occupied and one vacant natural orbital corresponding to the lone pairs (LPs). The formal Sb charge is, therefore, +1. Correspondingly, two unpaired electrons of Sb participate in the formation of two single covalent bonds (Sb−C and Sb−O). The Sb−N bonds are described as donor−acceptor interactions between the occupied LPs of nitrogens and vacant LP* of antimony. There is also an $O^- \rightarrow Sb^+$ coordination bond in ArSbO arising from the donation of the oxygen LP to the antimony LP* NBO. When it goes to the boron complexes, the NBO model of the Sb−O interactions changes. In **13** and **14**, the formal charges of these atoms are +2 and −2, respectively. One occupied and two vacant LPs are associated with the Sb atom, while the O atom possesses four occupied LPs. The $O^{2-} \rightarrow Sb^{2+}$ bond is a result of the electron density donation from two oxygen LPs (LP(3), >99% p and LP(4), 68% s, 32% p) to the antimony LP*(2) formed by the 5s (10%) and 5p (90%) Sb wave functions (Figure 9).

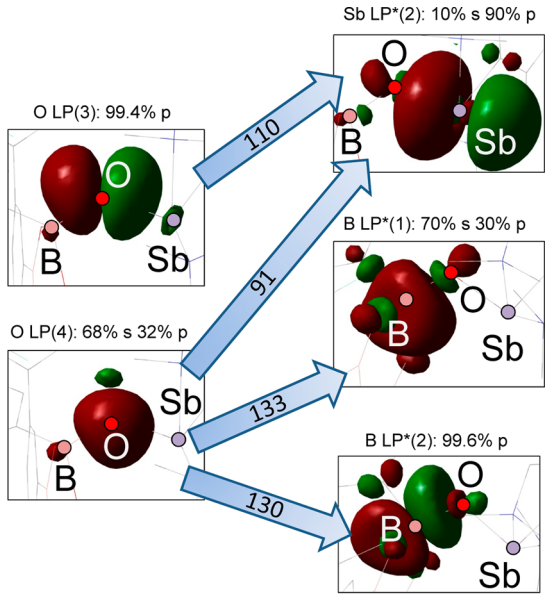

Figure 9. Occupied (left, isosurface 0.03 au) and vacant (right, isosurfaces 0.04 au) NBOs corresponding to the strongest donor−acceptor interactions in the Sb1−O1−B1 fragment of complex **13** (the atom notation corresponds to that in Figure 6). The corresponding energies obtained from the second-order perturbation theory analysis of the Fock matrix in the NBO basis (kcal/mol^{-1}) are shown on the arrows.

This description correlates well with the decrease in the positive DED between the O and Sb atoms (Figure 8) and the increase in the Sb charge (Table S2) upon going from ArSbO to **13** and **14**. As a result of the donor−acceptor interactions, the changes of atomic charges on formation of the boron complexes are much lower than those predicted by the frontier structures (Table S2). The NBO and Mulliken oxygen charges in **13** and **14** appear to be even less negative as compared to

DOI: 10.1021/acs.inorgchem.5b00893
Inorg. Chem. 2015, 54, 6010−6019

ArSbO. For the AIM charges an opposite trend is observed (Table S2), but this can be due to different shapes of the oxygen atomic basin in ArSbO and the boron derivatives. The $O^{2-} \rightarrow B$ bond in **13** and **14** is formed mainly by the donation of the oxygen LP(4) to the boron vacant LP*s (Figure 9). Notice that the NBO approach provides different frontier configurations for the B (ArSbO → B) atom in **13** and **14**. In the former compound, the boron atom bonded to the ArSbO fragment possesses three vacant LP*s, so its formal charge is +2, the two O neighboring atoms of the boroxine cycle representing monoanions. In **14**, boron forms three covalent bonds with the phenyl rings, so it is formally neutral. These models describe qualitatively the decrease in the B positive charge when going from **13** to **14** (Table S2). The frontier structures of the Sb−O−B fragment in **13**, **14**, and ArSbO suggested by the NBO analysis are summarized in Figure 10.

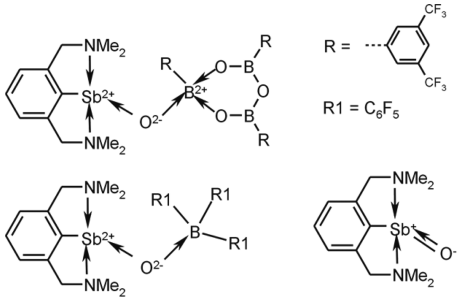

Figure 10. Frontier structures of the SbOB fragment in **13**, **14**, and ArSbO provided by the NBO analysis.

Notice, however, that the total NBO charges of the ArSb and $R_3B_3O_3$ fragments in **13** are, respectively, +1.95 and −0.73, which agrees well with the bipolar resonance $(ArSb)^+-O-(R_3B_3O_3)^-$ structure analogous to that of **14** and $Ph_3SbOB(C_6F_5)_3$.[19]

CONCLUSIONS

We have discovered unusual reactions between antimony oxide $(ArSbO)_2$ (**1**) and bismuth oxides $(ArBiO)_2$ (**2**) and boronic acids leading to the formation of ion pairs $[ArMR]^+$ $[R_4B_5O_6]^-$ (R = Ph, 4-$CF_3C_6H_4$, 4-BrC_6H_4). The pnictogen atoms (Sb or Bi) are arylated in the course of this procedure by respective boronic acids, which is, to the best of our knowledge, unprecedented feature in the chemistry of antimony and bismuth. This finding paves a new way for the preparation of N,C,N-chelated diorganoantimony (bismuth) compounds by simple treatment of easily accessible oxides **1** and **2** with commercially available boronic acids. This procedure seems to exhibit a tolerance toward functional groups attached to the migrating aryl group, which could be only hardly achieved using other conventional agents such as aryllithium compounds or Grignard reagents. A proposed reaction mechanism has been suggested, and compounds **10** and **13**, rare examples of adducts of monomeric antimony oxide with a Lewis acid, have been isolated. The structure of **13** was described in detail using theoretical approach and revealed partially different behavior in comparison with previously known complex $ArSbOB(C_6F_5)_3$ (**14**). The (Sb)O−B bond is predicted to be stronger in **13** than in **14**. However, the corresponding calculated dissociation energy appears to be higher for **14** due to larger reorganization energy of boroxine on formation of the **13** complex as compared to that of $B(C_6F_5)_3$. In the NBO-based frontier structures, the main difference is found at the boron atom, which forms three covalent bonds in **14**, while it carries +2 charge and is connected to the two neighboring monoanions of the boroxine cycle in **13**.

Investigation of the general applicability of here described synthetic protocol for arylation of N,C,N-chelated compounds in the field antimony and bismuth as well as other main group elements is currently underway.

EXPERIMENTAL SECTION

General Remarks. ^1H, ^{11}B, ^{13}C, and ^{19}F NMR spectra were recorded on Bruker Avance 500 MHz spectrometer or Bruker Ultrashield 400 MHz, using 5 mm tunable broad-band probe. Appropriate chemical shifts in ^1H and ^{13}C NMR spectra were related to the residual signals of the solvent ($CDCl_3$: $\delta(^1H)$ = 7.27 ppm and $\delta(^{13}C)$ = 77.23 ppm). ^{11}B NMR spectra were related to external standard $B(OMe)_3$ ($\delta(^{10}B)$ = 18.1 ppm). ^{19}F NMR chemical shifts were related according to the external standard CCl_3F $\delta(^{19}F)$ = 0.0 ppm. Elemental analyses were performed on an LECO−CHNS-932 analyzer. The starting compounds $(ArSbO)_2$[7] and $(ArBiO)_2$[8] were prepared according to literature procedures. Boronic acids were obtained from commercial suppliers and used as delivered.

General Procedure for the Preparation of 4−9. Each boronic acid (3 mol equiv) was added to the solution of respective heteroboroxine $ArM[(OBR)_2O]$ (M = Sb or Bi, R = Ph, 4-$CF_3C_6H_4$, 4-BrC_6H_4) in benzene (20 mL), and the resulting mixture was stirred under heating (60 °C) for additional 20 h. The reaction mixtures were evaporated in vacuo, and the observed residue was recrystallized (see detailed Discussion Section for each compound). All compounds were obtained as colorless solids.

*Compound $[ArSbPh]^+[Ph_4B_5O_6]^-$ (**4**).* 104 mg (0.86 mmol) of $PhB(OH)_2$ and 153 mg (0.29 mmol) $ArSb[(OBPh)_2O]$ gave after recrystallization from CH_2Cl_2/hexane compound **4**. Yield: 171 mg (71%). mp 217−219 °C. ^1H NMR ($CDCl_3$, 25 °C): δ = 1.74 (s, 6H, $(CH_3)_2N$), 2.48 (s, 6H, $(CH_3)_2N$), 3.55 (AB pattern, $^2J(^1H,^1H)$ = 15.2 Hz, 4H, CH_2N), 7.22−7.40 (m, 20H, Ar−H3,4,5, Sb-Ph, borate-Ph-H3,4,5), 8.12 (d, 8H, borate-Ph-H2,6); $^{13}C\{^1H\}$ NMR ($CDCl_3$, 25 °C): δ = 46.7 (s, $(CH_3)_2N$), 47.7 (s, $(CH_3)_2N$), 64.5 (s, CH_2N), 126.4, 127.2, 129.8, 130.1, 131.8, 132.2, 135.3 (s, Ar−C, Ph−C), 138.9 (Ph−C1-Sb), 139.4 (Ar−C1−Sb), 144.0 (s, Ar−C), (Ar−C1−B) not observed; $^{11}B\{^1H\}$ NMR ($CDCl_3$, 25 °C): δ = 0.37 (s, spiro-B), 27.8 (s(br), boroxine-B); positive-ion ESI-MS: m/z 389 $[ArSb(C_6H_5)]^+$ (100%); negative-ion ESI-MS: m/z 459 $[(C_6H_5)_4B_5O_6]^-$; anal. (%) calcd for $C_{42}H_{44}B_5N_2O_6Sb$ (848.63): C 59.4, H 5.2; found: C 59.6, H 5.3.

*Compound $[ArSb(4\text{-}CF_3C_6H_4)]^+[(4\text{-}CF_3C_6H_4)_4B_5O_6]^-$ (**5**).* 234 mg (1.23 mmol) of (4-$CF_3C_6H_4$)$B(OH)_2$ and 276 mg (0.41 mmol) $ArSb[(OB(4\text{-}CF_3C_6H_4))_2O]$ gave after recrystallization from CH_2Cl_2/hexane compound **5**. Yield: 288 mg (59%). mp 79−83 °C (dec). ^1H NMR ($CDCl_3$, 25 °C): δ = 1.81 (s, 6H, $(CH_3)_2N$), 2.47 (s, 6H, $(CH_3)_2N$), 3.58 (AX pattern, $^2J_{H-H}$ = 15.2 Hz, 4H, CH_2N), 7.24 (d, 2H, Ar−H3,5), 7.31 (m(br), 1H, Ar−H4), 7.49 (d, 2H, Sb-4-$CF_3C_6H_4$), 7.57 (d, 8H, borate-4-$CF_3C_6H_4$), 7.65 (d, 2H, Sb-4-$CF_3C_6H_4$), 8.20 (d, 8H, borate-4-$CF_3C_6H_4$); $^{13}C\{^1H\}$ NMR ($CDCl_3$, 25 °C): δ = 47.1 (s, $(CH_3)_2N$), 48.0 (s, $(CH_3)_2N$), 64.8 (s, CH_2N), 123.4 (q, $^1J(^{19}F,^{13}C)$ = 270.5 Hz, CF_3), 124.0 (m, C_6H_4), 124.7 (q, $^1J(^{19}F,^{13}C)$ = 272.3 Hz, CF_3), 126.9 (overlap of two signals, Ar−C and C_6H_4), 127.1 (m, C_6H_4), 131.7 (q, $^2J(^{19}F,^{13}C)$ = 32.0 Hz, C_{ipso}-CF_3), 133.0 (s, Ar−C), 134.3 (q, $^2J(^{19}F,^{13}C)$ = 33.4 Hz, C_{ipso}-CF_3), 135.3 (m, C_6H_4), 138.4 (C_6H_4−C1-Sb), 142.8 (Ar−C1−Sb), 144.0 (s, Ar−C), (C_6H_4−C1-B) not observed; $^{11}B\{^1H\}$ NMR ($CDCl_3$, 25 °C): δ = 0.34 (s, spiro-B), 27.9 (s(br), boroxine-B); $^{19}F\{^1H\}$ NMR ($CDCl_3$, 25 °C): δ = −62.5 (s, CF_3), −63.4 (s, CF_3); positive-ion ESI-MS: m/z 457 $[ArSb(4\text{-}CF_3C_6H_4)]^+$ (100%); negative-ion ESI-MS: m/z 731 $[(4\text{-}CF_3C_6H_4)_4B_5O_6]^-$; anal. (%) calcd for $C_{47}H_{39}B_5F_{15}N_2O_6Sb$ (1188.63): C 47.5, H 3.3; found: C 47.7, H 3.6.

*Compound $[ArSb(4\text{-}BrC_6H_4)]^+[(4\text{-}BrC_6H_4)_4B_5O_6]^-$ (**6**).* 153 mg (0.76 mmol) of (4-BrC_6H_4)$B(OH)_2$ and 176 mg (0.25 mmol) $ArSb[(OB(4\text{-}$

DOI: 10.1021/acs.inorgchem.5b00893
Inorg. Chem. 2015, 54, 6010−6019

$BrC_6H_4))_2O$] gave after recrystallization from $CHCl_3$/hexane compound **6**. Yield: 183 mg (58%). mp 91 °C (dec). ^{1}H NMR ($CDCl_3$, 25 °C): δ = 1.84 (s, 6H, $(CH_3)_2N$), 2.48 (s, 6H, $(CH_3)_2N$), 3.57 (AB pattern, $^2J(^1H,^1H)$ = 15.2 Hz, 4H, CH_2N), 7.04 (s(br), 1H, Ar−H4), 7.25 (d, 2H, Ar−H3,5), 7.41 (d, 8H, borate-4-BrC_6H_4), 7.50 (d, 2H, Sb-4-BrC_6H_4), 7.55 (d, 2H, Sb-4-BrC_6H_4), 7.91 (d, 8H, borate-4-BrC_6H_4); $^{13}C\{^1H\}$ NMR ($CDCl_3$, 25 °C): δ = 47.1 (s, $(CH_3)_2N$), 47.9 (s, $(CH_3)_2N$), 64.8 (s, CH_2N), 125.0 (s, C_{ipso}-Br), 126.8 (s, Ar−C), 127.6 (s, C_{ipso}-Br), 128.5, 130.5, 132.8, 133.7, 137.0 (s, Ar−C and C_4H_6), 137.3 (C_6H_4−C1-Sb), 138.8 (Ar−C1−Sb), 144.0 (s, Ar−C), (C_6H_4−C1-B) not observed; $^{11}B\{^1H\}$ NMR ($CDCl_3$, 25 °C): δ = 0.2 (s, spiro-B), 29.8 (s(br), boroxine-B); positive-ion ESI-MS: m/z 467 $[ArSb(4\text{-}BrC_6H_4)]^+$ (100%); negative-ion ESI-MS: m/z 771 $[(4\text{-}BrC_6H_4)_4B_5O_6]^-$; anal. (%) calcd for $C_{42}H_{39}B_5Br_5N_2O_6Sb$ (1243.11): C 40.6, H 3.2; found: C 40.8, H 3.5.

*Compound [ArBiPh]$^+$[Ph$_4$B$_5$O$_6$]$^-$ (**7**).* 117 mg (0.96 mmol) of $PhB(OH)_2$ and 200 mg (0.32 mmol) ArBi[$(OBPh)_2O$] gave after recrystallization from CH_2Cl_2/hexane compound **7**. Yield: 162 mg (54%). mp 216−218 °C. ^{1}H NMR ($CDCl_3$, 25 °C): δ = 1.89 (s, 6H, $(CH_3)_2N$), 2.54 (s, 6H, $(CH_3)_2N$), 3.59 (AX pattern, $^2J(^1H,^1H)$ = 14.8 Hz, 4H, CH_2N), 7.20−7.55 (m, 18H, Ar−H3,4,5, Bi-Ph-H3,4,5, borate-Ph-H3,4,5), 7.74 (d, 2H, Bi-Ph-H2,6), 8.07 (d, 8H, borate-Ph-H2,6); $^{13}C\{^1H\}$ NMR ($CDCl_3$, 25 °C): δ = 47.5 (s, $(CH_3)_2N$), 48.1 (s, $(CH_3)_2N$), 68.1 (s, CH_2N), 127.4, 128.7, 130.1, 130.4, 130.5, 132.3, 135.3, 137.3 150.1 (Ar−C, Ph−C), 179.8 (Ph−C1-Bi), 184.6 (Ar−C1−Bi), (Ph−C1-B) not observed; $^{11}B\{^1H\}$ NMR ($CDCl_3$, 25 °C): δ = 0.42 (s, spiro-B), 28.3 (s(br), boroxine-B); positive-ion ESI-MS: m/z 477 $[ArBi(C_6H_5)]^+$ (100%); negative-ion ESI-MS: m/z 459 $[(C_6H_5)_4B_5O_6]^-$; anal (%) calcd for $C_{42}H_{44}B_5BiN_2O_6$ (935.86): C 53.9, H 4.7; found: C 53.6, H 5.0.

*Compound [ArBi(4-CF$_3$C$_6$H$_4$)]$^+$[(4-CF$_3$C$_6$H$_4$)$_4$B$_5$O$_6$]$^-$ (**8**).* 157 mg (0.83 mmol) of $(4\text{-}CF_3C_6H_4)B(OH)_2$ and 210 mg (0.28 mmol) ArBi[$(OB(4\text{-}CF_3C_6H_4))_2O$] gave after recrystallization from CH_2Cl_2/hexane compound **8**. Yield: 236 mg (67%). mp 202−205 °C. ^{1}H NMR ($CDCl_3$, 25 °C): δ = 2.05 (s, 6H, $(CH_3)_2N$), 2.55 (s, 6H, $(CH_3)_2N$), 3.68 (AX pattern, $^2J_{H-H}$ = 15.2 Hz, 4H, CH_2N), 7.57 (m, 11H, Ar−H3,4,5, borate-4-$CF_3C_6H_4$), 7.78 (d, 2H, Bi-4-$CF_3C_6H_4$), 7.84 (d, 2H, Bi-4-$CF_3C_6H_4$), 8.19 (d, 8H, borate-4-$CF_3C_6H_4$); $^{13}C\{^1H\}$ NMR ($CDCl_3$, 25 °C): δ = 47.8 (s, $(CH_3)_2N$), 48.0 (s, $(CH_3)_2N$), 67.9 (s, CH_2N), 123.7 (q, $^1J(^{19}F,^{13}C)$ = 273.7 Hz, CF_3), 124.1 (m, C_6H_4), 124.6 (q, $^1J(^{19}F,^{13}C)$ = 273.7 Hz, CF_3), 128.5 (s, Ar−C), 129.2 (m, C_6H_4), 131.4 (s, Ar−C), 132.0 (q, $^2J(^{19}F,^{13}C)$ = 31.8 Hz, C_{ipso}-CF_3), 133.0 (q, $^2J(^{19}F,^{13}C)$ = 33.0 Hz, C_{ipso}-CF_3), 135.3 (m, C_6H_4), 137.5 (m, C_6H_4), 149.8 (s, Ar−C), 181.8 (C_6H_4−C1-Bi), 182.0 (Ar−C1−Bi), (C_6H_4−C1-B) not observed; $^{11}B\{^1H\}$ NMR ($CDCl_3$, 25 °C): δ = 0.46 (s, spiro-B), 28.8 (s(br), boroxine-B); $^{19}F\{^1H\}$ NMR ($CDCl_3$, 25 °C): δ = −62.6 (s, CF_3), −63.3 (s, CF_3); positive-ion ESI-MS: m/z 545 $[ArBi(4\text{-}CF_3C_6H_4)]^+$ (100%); negative-ion ESI-MS: m/z 731 $[(4\text{-}CF_3C_6H_4)_4B_5O_6]^-$; elemental analysis (%) calcd for $C_{47}H_{39}B_5BiF_{15}BiN_2O_6$ (1275.86): C 44.3, H 3.1; found: C 44.6, H 3.2.

*Compound [ArBi(4-BrC$_6$H$_4$)]$^+$[(4-BrC$_6$H$_4$)$_4$B$_5$O$_6$]$^-$ (**9**).* 142 mg (0.71 mmol) of $(4\text{-}BrC_6H_4)B(OH)_2$ and 184 mg (0.24 mmol) ArBi[$(OB(4\text{-}BrC_6H_4))_2O$] gave after recrystallization from $CHCl_3$/hexane compound **9**. Yield: 216 mg (69%). mp 85 °C (dec). ^{1}H NMR ($CDCl_3$, 25 °C): δ = 2.04 (s, 6H, $(CH_3)_2N$), 2.57 (s, 6H, $(CH_3)_2N$), 3.66 (AB pattern, $^2J(^1H,^1H)$ = 14.8 Hz, 4H, CH_2N), 7.41 (d, 8H, borate-4-BrC_6H_4), 7.55 (m, 4H, Ar−H3,5, Bi-4-BrC_6H_4), 7.64 (m, 1H, Ar−H4), 7.68 (d, 2H, Bi-4-BrC_6H_4), 7.90 (d, 8H, borate-4-BrC_6H_4); $^{13}C\{^1H\}$ NMR ($CDCl_3$, 25 °C): δ = 47.8 (s, $(CH_3)_2N$), 48.1 (s, $(CH_3)_2N$), 67.9 (s, CH_2N), 125.2 (s, C_{ipso}-Br), 126.0 (s, C_{ipso}-Br), 128.5, 129.1, 130.7, 131.1, 135.8, 136.9, 138.7, 149.9 (s, Ar−C and C_6H_4), 176.8 (C_6H_4−C1-Bi), 182.7 (Ar−C1−Bi), (C_6H_4−C1-B) not observed; $^{11}B\{^1H\}$ NMR ($CDCl_3$, 25 °C): δ = 0.22 (s, spiro-B), 28.6 (s(br), boroxine-B); positive-ion ESI-MS: m/z 555 $[ArBi(4\text{-}BrC_6H_4)]^+$ (100%); negative-ion ESI-MS: m/z 771 $[(4\text{-}BrC_6H_4)_4B_5O_6]^-$; anal. (%) calcd for $C_{42}H_{39}B_5BiBr_5N_2O_6$ (1330.34): C 37.9, H 3.0; found: C 38.2, H 3.3.

*Compound ArSb[(OB-3,5-(CF$_3$)$_2$C$_6$H$_3$)$_2$O] (**11**).* 391 mg (1.52 mmol) of $3,5\text{-}(CF_3)_2C_6H_3B(OH)_2$ and oxide **1** (250 mg, 0.38 mmol) were mixed in dichloromethane and stirred for 3 h at room temperature (r.t.). The reaction mixture was evaporated in vacuo, and the crude product was recrystallized from CH_2Cl_2/hexane to give **11** as colorless solid. Yield: 461 mg (75%). mp 187−190 °C. ^{1}H NMR ($CDCl_3$, 25 °C): δ = 2.10 (s(br), 6H, $(CH_3)_2N$), 2.84 (s(br), 6H, $(CH_3)_2N$), 3.88 (AX pattern, $^2J(^1H,^1H)$ = 13.6 Hz, 4H, CH_2N), 7.09 (d, 2H, Ar−H3,5), 7.23 (t, 1H, Ar−H4), 7.90 (s, 2H, 3,5-$(CF_3)_2C_6H_3$−H4), 8.39 (s, 4H, 3,5-$(CF_3)_2C_6H_3$−H2,6); $^{13}C\{^1H\}$ NMR ($CDCl_3$, 25 °C): δ = $(CH_3)_2N$ not observed due to the significant broadening, 63.2 (s, CH_2N), 123.8 (m, 3,5-$(CF_3)_2C_6H_3$−C4), 124.0 (q, $^1J(^{19}F,^{13}C)$ = 272.9 Hz, CF_3), 126.6 (s, Ar−C3,5), 130.0 (s, Ar−C4), 130.7 (q, $^2J(^{19}F,^{13}C)$ = 32.8 Hz, 3,5-$(CF_3)_2C_6H_3$−C3,5), 134.5 (m, 3,5-$(CF_3)_2C_6H_3$−C2,6), 147.2 (s, Ar−C2,6), 154.8 (s, Ar−C1), (C_{ipso}-B) not observed; $^{11}B\{^1H\}$ NMR ($CDCl_3$, 25 °C): δ = 27.3 (s(br)); $^{19}F\{^1H\}$ NMR ($CDCl_3$, 25 °C): δ = −62.9 (s, CF_3); anal. (%) calcd for $C_{28}H_{25}B_2F_{12}N_2O_3Sb$ (808.88): C 41.6, H 3.1; found: C 41.9, H 3.4.

*Compound ArBi[(OB-3,5-(CF$_3$)$_2$C$_6$H$_3$)$_2$O] (**12**).* 180 mg (0.70 mmol) of $3,5\text{-}(CF_3)_2C_6H_3B(OH)_2$ and oxide **2** (146 mg, 0.18 mmol) were mixed in dichloromethane and stirred for 3 h at r.t. The reaction mixture was evaporated in vacuo, and the crude product was recrystallized from CH_2Cl_2/hexane to give **12** as colorless solid. Yield: 201 mg (64%). mp 166−169 °C. ^{1}H NMR ($CDCl_3$, 25 °C): δ = 2.18 (s, 6H, $(CH_3)_2N$), 2.93 (s(br), 6H, $(CH_3)_2N$), 4.03 (AX pattern, $^2J(^1H,^1H)$ = 13.6 Hz, 4H, CH_2N), 7.32 (t, 1H, Ar−H4), 7.47 (d, 2H, Ar−H3,5), 7.87 (s, 2H, 3,5-$(CF_3)_2C_6H_3$−H4), 8.40 (s, 4H, 3,5-$(CF_3)_2C_6H_3$−H2,6); $^{13}C\{^1H\}$ NMR ($CDCl_3$, 25 °C): δ = 42.4 (s, $(CH_3)_2N$), 46.0 (s, $(CH_3)_2N$), 65.6 (s, CH_2N), 123.3 (m, 3,5-$(CF_3)_2C_6H_3$−C4), 124.1 (q, $^1J(^{19}F,^{13}C)$ = 273.3 Hz, CF_3), 128.8 (s, Ar−C3,5), 129.4 (s, Ar−C4), 130.5 (q, $^2J(^{19}F,^{13}C)$ = 32.6 Hz, 3,5-$(CF_3)_2C_6H_3$−C3,5), 134.6 (m, 3,5-$(CF_3)_2C_6H_3$−C2,6), 152.2 (s, Ar−C2,6), 205.9 (s, Ar−C1), (C_{ipso}-B) not observed;$^{11}B\{^1H\}$ NMR ($CDCl_3$, 25 °C): δ = 26.8 (s(br)); $^{19}F\{^1H\}$ NMR ($CDCl_3$, 25 °C): δ = −62.9 (s, CF_3); anal. (%) calcd for $C_{28}H_{25}B_2BiF_{12}N_2O_3$ (896.11): C 37.5, H 2.8; found: C 37.8, H 3.0.

*Compound [ArSbO-(OB-3,5-(CF$_3$)$_2$C$_6$H$_3$)$_3$] (**13**).* 69 mg (0.27 mmol) of $3,5\text{-}(CF_3)_2C_6H_3B(OH)_2$ and compound **11** 215 mg (0.27 mmol) were mixed in dichloromethane and stirred for 3 h at r.t. The reaction mixture was evaporated in vacuo, and the crude product was recrystallized from CH_2Cl_2/hexane to give **13** as colorless solid. Yield: 226 mg (81%). mp 162−164 °C. ^{1}H NMR ($CDCl_3$, 25 °C): δ = 2.54 (s, 6H, $(CH_3)_2N$), 2.67 (s, 6H, $(CH_3)_2N$), 3.94 (AB pattern, $^2J(^1H,^1H)$ = 14.8 Hz, 4H, CH_2N), 7.24 (d, 2H, Ar−H3,5), 7.43 (t, 1H, Ar−H4), 7.62 (s, 1H, ArSbO-B(3,5-$(CF_3)_2C_6H_3$)-H4), 8.00 (s, 2H, boroxine-(3,5-$(CF_3)_2C_6H_3$)-H4), 8.09 (s, 2H, ArSbO-B(3,5-$(CF_3)_2C_6H_3$)-H2,6), 8.52 (s, 4H, boroxine-(3,5-$(CF_3)_2C_6H_3$)-H2,6); $^{13}C\{^1H\}$ NMR ($CDCl_3$, 25 °C): δ = 45.9 (s, $(CH_3)_2N$), 46.1 (s, $(CH_3)_2N$), 65.0 (s, CH_2N), 120.0 (m, ArSbO-B(3,5-$(CF_3)_2C_6H_3$)-C4), 121.8 (q, $^1J(^{19}F,^{13}C)$ = 273.0 Hz, CF_3), 124.0 (q, $^1J(^{19}F,^{13}C)$ = 271.8 Hz, CF_3), 124.4 (m, boroxine-(3,5-$(CF_3)_2C_6H_3$)-C4), 125.9 (s, Ar−C3,5), 129.8 (q, $^2J(^{19}F,^{13}C)$ = 32.6 Hz, ArSbO-B(3,5-$(CF_3)_2C_6H_3$)-C3,5), 130.9 (q, $^2J(^{19}F,^{13}C)$ = 32.9 Hz, boroxine-(3,5-$(CF_3)_2C_6H_3$)-C3,5), 131.4 (m, ArSbO-B(3,5-$(CF_3)_2C_6H_3$)-C2,6), 132.2 (s, Ar−C4), 134.8 (m, boroxine-(3,5-$(CF_3)_2C_6H_3$)-C2,6), 144.6 (s, Ar−C2,6), 148.3 (s, Ar−C1), (C_{ipso}-B) not observed; $^{11}B\{^1H\}$ NMR ($CDCl_3$, 25 °C): δ = 3.0 (s, spiro-B), 27.9 (s(br), boroxine-B); $^{19}F\{^1H\}$ NMR ($CDCl_3$, 25 °C): δ = −62.5 (s, CF_3), −62.8 (s, CF_3); elemental analysis (%) calcd for $C_{36}H_{29}B_3F_{18}N_2O_4Sb$ (1049.80): C 41.2, H 2.8; found: C 40.9, H 2.9.

Density Functional Theory Calculations. The geometry optimization and NBO analysis[22] of ArSbO and complexes **13** and **14** were performed at the M062X/DGDZVP level of theory with the Gaussian09 package.[23] The quantum theory of atoms in molecules (QTAIM)[24] was employed to investigate the electron density topologies and charge distribution on the basis of the AIMALL[25] and Multiwfn[26] codes. The EDA for **13** and **14** was performed with use of the Morokuma approach.[21] The computational details are given in Supporting Information.

X-ray Diffraction Analyses. Suitable single crystals of **4**, **7**, **10**, **11**, and **13** were mounted on a glass fiber with an oil and measured on

DOI: 10.1021/acs.inorgchem.5b00893
Inorg. Chem. 2015, 54, 6010−6019

four-circle diffractometer KappaCCD with CCD area detector by monochromatized Mo Kα radiation (λ = 0.710 73 Å). Corresponding crystallographic data are given in Supporting Information, Table S4. The numerical[27] absorption correction from crystal shape was applied for all crystals. The structures were solved by the direct method (SIR92[28]) and refined by a full matrix least-squares procedure based on F^2 (SHELXL97[29]). Hydrogen atoms were mostly localized on a difference Fourier map; however, to ensure the uniformity of treatment of crystal, all hydrogen were recalculated into idealized positions (riding model) and assigned temperature factors $H_{iso}(H)$ = 1.2 U_{eq}(pivot atom) or of 1.5U_{eq} for the methyl moiety with C−H = 0.96, 0.98, and 0.93 Å for methyl, methylene, and hydrogen atoms in aromatic rings, respectively. In the crystal structure of compounds **7** and **13** water molecules were present in the unit cell, in the structure of **7** hydrogen atoms one of these water molecules were treated to obtain the best hydrogen bond connectivity, while in **13** water molecules were masked by the Squeeze program, and the remaining electron density was eight electrons per unit cell.[30] In compound **11**, one of the fluorine atoms is slightly disordered and remained untreated; on the other hand, all the fluorine atoms in **13** and **10** were split into two positions to model theirs disorders. These splitting procedures were performed using SHELXL2013 program and SADI procedures. Moreover in the crystal structure of **10**, 92 electrons per unit cell were masked by the PLATON/SQUEZZE program[30] revealing the occupancy of two dichloromethane molecules per unit cell. The cavity originated in the structure of **10** is shown in Figure S2. Additional crystallographic information is available in the Supporting Information.

■ ASSOCIATED CONTENT

Supporting Information

NMR spectra, illustrated cavity of **10**, details of computational analysis including tabulated calculated bond lengths, BCP electron densities, ratio of potential energy density/kinetic energy density, NBO, Mulliken, and AIM charges, energy decomposition analysis, and crystallographic data. All crystal data and structure refinement, atomic coordinates, anisotropic displacement parameters, and geometric data for studied compounds (cif files). Additional references. The Supporting Information is available free of charge on the ACS Publications website at DOI: 10.1021/acs.inorgchem.5b00893. Crystallographic data for structural analysis has been deposited with the Cambridge Crystallographic Data Centre, CCDC Nos. 1059935−1059939. Copies of this information may be obtained free of charge from The Director, CCDC, 12 Union Road, Cambridge CB2 1EY, U.K. (Fax: +44−1223−336033; E-mail: deposit@ccdc.cam.ac.uk or www:http://www.ccdc.cam.ac.uk).

■ AUTHOR INFORMATION

Corresponding Authors

*Fax: +420466037068. Phone: +420466037163. E-mail: libor.dostal@upce.cz. (L.D.)

*E-mail: sketkov@iomc.ras.ru. (S.K.)

Notes

The authors declare no competing financial interest.

■ ACKNOWLEDGMENTS

The authors thank the Grant agency of the Czech Republic Project No. P207/13-00289S. The DFT part of this work was supported by the Russian Science Foundation (Project 14-13-00832).

■ REFERENCES

(1) For selected examples see: (a) Hall, D. G.; Frye, G. C. In *Boronic Acids;* Wiley-VCH: Weinheim, Germany, 2005. (b) Korich, A. L.; Iovine, P. M. *Dalton. Trans.* **2010**, *39*, 1423. (b) Westcott, S. A. *Angew. Chem., Int. Ed.* **2010**, *49*, 9045. (c) Cote, A. P.; Benin, A. I.; Ockwig, N. W.; O'Keeffe, M.; Matzger, A. J.; Yaghi, O. M. *Science* **2005**, *310*, 1166. (d) Cambell, N. L.; Clowes, R.; Ritchie, L. K.; Cooper, A. I. *Chem. Mater.* **2009**, *21*, 204. (e) Cao, D.; Lan, J.; Wang, W.; Smith, B. *Angew. Chem., Int. Ed.* **2009**, *48*, 4730. (f) El-Kaderi, H. M.; Hunt, J. R.; Mendoza-Cortes, J. L.; Cote, A. P.; Taylor, R. E.; O'Keeffe, M.; Yaghi, M. *Science* **2007**, *316*, 268. (h) Han, S. S.; Furukava, H.; Yaghi, O. M.; Goddard, W. A. *J. Am. Chem. Soc.* **2008**, *130*, 11580. (i) Tilford, R. W.; Gemmill, W. R.; zur Loye, H.-C.; Lavigne, J. J. *Chem. Mater.* **2008**, *20*, 2741. (j) Mastalerz, M. *Angew. Chem., Int. Ed.* **2008**, *120*, 445. (k) Graham, T. J. A.; Shields, J. D.; Doyle, A. G. *Chem. Sci.* **2011**, *2*, 980. (l) Xu, L.; Li, B. J.; Wu, Z. H.; Lu, X. Y.; Guan, B. T.; Wang, B. Q.; Zhao, K. Q.; Shi, Z. J. *Org. Lett.* **2010**, *12*, 884. (m) Song, Z. Z.; Wong, H. N. C.; Yang, Y. *Pure Appl. Chem.* **1996**, *68*, 723. (n) Tokunaga, Y. *Heterocycles* **2013**, *87*, 991. (o) Clair, S.; Abel, M.; Porte, L. *Chem. Commun.* **2014**, *50*, 9627. (p) Smith, M. K.; Northrop, B. H. *Chem. Mater.* **2014**, *26*, 3781. (q) Ito, M.; Itazaki, M.; Nakazawa, H. *J. Am. Chem. Soc.* **2014**, *136*, 6183.

(2) (a) Ma, X.; Yang, Z.; Wang, X.; Roesky, H. W.; Wu, F.; Zhu, H. *Inorg. Chem.* **2011**, *50*, 2010. (b) Yang, Z.; Ma, X.; Oswald, R. B.; Roesky, H. W.; Noltemeyer, M. *J. Am. Chem. Soc.* **2006**, *128*, 12406. (c) Brown, P.; Mahon, M. F.; Molloy, K. C. *Dalton Trans.* **1992**, 3503. (c) Vargas, G.; Hernández, I.; Höpfl, H.; Ochoa, M. E.; Castillo, D.; Farfán, N.; Santillan, R.; Gómez, E. *Inorg. Chem.* **2004**, *43*, 8490. (e) Yang, Z.; Hao, P.; Liu, Z.; Ma, X.; Roesky, H. W.; Li, J. *J. Organomet. Chem.* **2014**, *751*, 788. (f) Hao, P. F.; Yang, Z.; Ma, X. L.; Li, J. R. *Chin. J. Inorg. Chem.* **2013**, *29*, 1909.

(3) (a) Liu, W. J.; Pink, M.; Lee, D. *J. Am. Chem. Soc.* **2009**, *131*, 8703. (b) Avent, A. G.; Lawrence, S. E.; Meehan, M. M.; Russell, T. G.; Spalding, T. R. *Collect. Czech. Chem. Commun.* **2002**, *67*, 1051.

(4) (a) Mairychová, B.; Svoboda, T.; Štěpnička, P.; Růžička, A.; Havenith, R. W. A.; Alonso, M.; De Proft, F.; Jambor, R.; Dostál, L. *Inorg. Chem.* **2013**, *52*, 1424. (b) Kořenková, M.; Mairychová, B.; Růžička, A.; Jambor, R.; Dostál, L. *Dalton Trans.* **2014**, *43*, 7096. (c) Mairychová, B.; Štěpnička, P.; Růžička, A.; Dostál, L.; Jambor, R. *Organometallics* **2014**, *33*, 3021.

(5) Kořenková, M.; Mairychová, B.; Jambor, R.; Růžičková, Z.; Dostál, L. *Inorg. Chem. Commun.* **2014**, *47*, 128.

(6) Kořenková, M.; Erben, M.; Jambor, R.; Růžička, A.; Dostál, L. *J. Organomet. Chem.* **2014**, *772*−*773*, 287.

(7) Dostál, L.; Jambor, R.; Růžička, A.; Erben, M.; Jirásko, R.; Černošková, Z.; Holeček, J. *Organometallics* **2009**, *28*, 2633.

(8) Fridrichová, A.; Svoboda, T.; Jambor, R.; Padělková, Z.; Růžička, A.; Erben, M.; Jirásko, R.; Dostál, L. *Organometallics* **2009**, *28*, 5522.

(9) Jirásko, R.; Holčapek, M. *Mass Spectrom. Rev.* **2011**, *30*, 1013.

(10) (a) Nishihara, Y.; Nara, K.; Osakada, K. *Inorg. Chem.* **2002**, *41*, 4090. (b) Nishihara, Y.; Nara, K.; Nishide, Y.; Osakada, K. *Dalton Trans.* **2004**, 1366.

(11) (a) Pyykkö, P.; Atsumi, M. *Chem.—Eur. J.* **2009**, *15*, 186. (b) Pyykkö, P.; Atsumi, M. *Chem.—Eur. J.* **2009**, *15*, 12770. (c) Pyykkö, P.; Riedel, S.; Patzschke, M. *Chem.—Eur. J.* **2005**, *11*, 3511.

(12) Dostál, L.; Jambor, R.; Jirásko, R.; Padělková, Z.; Růžička, A.; Holeček, J. *J. Organomet. Chem.* **2010**, *695*, 392.

(13) Casely, I. J.; Ziller, J. W.; Mincher, B. J.; Evans, W. J. *Inorg. Chem.* **2011**, *50*, 1513.

(14) Dostál, L.; Jambor, R.; Růžička, A.; Jirásko, R.; Holeček, J.; De Proft, F. *Dalton Trans.* **2011**, *40*, 8922.

(15) Möhlmann, L.; Wendt, O. F.; Johnson, M. T. *Acta Crystallogr., Sect. E: Struct. Rep. Online* **2011**, *E67*, m719.

(16) (a) Snyder, H. R.; Konecky; Milton, S.; Lennarz, W. *J. Am. Chem. Soc.* **1958**, *80*, 3611. (b) Yalpani, M.; Boese, R. *Chem. Ber.* **1983**, *116*, 3347. (c) Beckett, M. A.; Strickland, G. C.; Varma, K. S.; Hibbs, D. E.; Hursthouse, M. B.; Malik, K. M. A. *Polyhedron* **1995**, *14*, 2623. (d) Beckett, M. A.; Strickland, G. C.; Varma, K. S.; Hibbs, D. E.;

DOI: 10.1021/acs.inorgchem.5b00893
Inorg. Chem. 2015, 54, 6010−6019

Hursthouse, M. B.; Malik, K. M. A. *J. Organomet. Chem.* **1997**, *535*, 33. (e) Beckett, M. A.; Hibbs, D. E.; Hursthouse, M. B.; Owen, P.; Malik, K. M.; Varma, K. S. *Main Group Chem.* **1998**, *2*, 251. (f) Beckett, M. A.; Brassington, D. S.; Owen, P.; Hursthouse, M. B.; Light, M. E.; Malik, K. M. A.; Varma, K. S. *J. Organomet. Chem.* **1999**, *585*, 7. (g) Wu, Q. G.; Wu, G.; Brancaleon, L.; Wang, S. *Organometallics* **1999**, *18*, 2553. (h) Beckmann, J.; Dakternieks, D.; Duthie, A.; Lim, A. E. K.; Tiekink, E. R. T. *J. Organomet. Chem.* **2001**, *633*, 149. (i) McKinley, N. F.; O'Shea, D. F. *J. Org. Chem.* **2004**, *69*, 5087. (j) Beckett, M. A.; Coles, S. J.; Light, M. E.; Fischer, L.; Stiefvater-Thomas, B. M.; Varma, K. S. *Polyhedron* **2006**, *25*, 1011. (k) Pearson, W. H.; Lin, S.; Iovine, P. M. *Acta Crystallogr.* **2008**, *E64*, o235. (l) Zhang, D.; Li, J.; Dong, X.; Zhou, X.; Yang, Z.; Roesky, H. W. *Z. Naturforsch.* **2013**, *B68*, 453. (m) Saha, S.; Kottalanka, R. K.; Panda, T. K.; Harms, K.; Dehnen, S.; Nayek, H. P. *J. Organomet. Chem.* **2013**, *745*−*746*, 329.

(17) For example see: (a) Yao, S.; Brym, M.; van Wüllen, C.; Driess, M. *Angew. Chem., Int. Ed.* **2007**, *46*, 4159. (b) Xiong, Y.; Yao, S.; Irran, E.; Driess, M. *Chem.—Eur. J.* **2011**, *17*, 11274. (c) Yao, S.; Xiong, Y.; Wang, W.; Driess, M. *Chem.—Eur. J.* **2011**, *17*, 4890. (d) Epping, J. D.; Yao, S.; Karni, M.; Apeloig, Y.; Driess, M. *J. Am. Chem. Soc.* **2010**, *132*, 5443. (e) Xiong, Y.; Yao, S.; Driess, M. *Dalton Trans.* **2010**, *39*, 9282. (f) Ghadwal, R. S.; Azhakar, R.; Roesky, H. W.; Pröpper, K.; Dittrich, B.; Goedecke, C.; Frenking, G. *Chem. Commun.* **2012**, *48*, 8186.

(18) (a) Dostál, L.; Jambor, R.; Růžička, A.; Lyčka, A.; Brus, J.; De Proft, F. *Organometallics* **2008**, *27*, 6059. (b) Dostál, L.; Jambor, R.; Růžička, A.; Jirásko, R.; Lochař, V.; Beneš, L.; De Proft, F. *Inorg. Chem.* **2009**, *48*, 10495. (c) Dostál, L.; Jambor, R.; Růžička, A.; Jirásko, R.; Černošková, E.; Beneš, L.; De Proft, F. *Organometallics* **2010**, *29*, 4486. (d) Šimon, P.; Jambor, R.; Růžička, A.; Lyčka, A.; De Proft, F.; Dostál, L. *Dalton Trans.* **2012**, *41*, 5140.

(19) Kather, R.; Svoboda, T.; Wehrhahn, M.; Rychagova, E.; Lork, E.; Dostál, L.; Ketkov, S.; Beckmann, J. *Chem. Commun.* **2015**, DOI: 10.1039/c5cc00738k.

(20) (a) Espinosa, E.; Alkorta, I.; Elguero, J.; Molins, E. *J. Chem. Phys.* **2002**, *117*, 5529−5542. (b) Gibbs, G. V.; Cox, D. F.; Crawford, T. D.; Rosso, K. M.; Ross, N. L.; Downs, R. T. *J. Chem. Phys.* **2006**, *124*, 084704−1−084704−8.

(21) (a) Morokuma, K. *J. Chem. Phys.* **1971**, *55*, 1236. (b) Morokuma, K.; Kitaura, K. In *Chemical Applications of Atomic and Molecular Electronic Potentials;* Politzer, P., Truhlar, D. G., Eds.; Plenum: New York, 1981; p 215. (c) Ziegler, T.; Rauk, A. *Theor. Chim. Acta* **1977**, *46*, 1. (d) Ziegler, T.; Rauk, A. *Inorg. Chem.* **1979**, *18*, 1755.

(22) (a) Reed, A. E.; Curtiss, L. A.; Weinhold, F. *Chem. Rev.* **1988**, *88*, 899. (b) Weinhold, F.; Carpenter, J. E. In *The Structure of Small Molecules and Ions;* Naaman, R., Vager, Z., Ed.; Plenum: New York, 1988; p 227.

(23) *Gaussian 09,* Revision B.01; Frisch, M. J., et al. Gaussian, Inc.: Wallingford, CT, 2010.

(24) (a) Cortés-Guzmàn, F.; Bader, R. F. W. *Coord. Chem. Rev.* **2005**, *249*, 633. (b) Bader, R. F. W. *A Quantum Theory;* Oxford University Press: Oxford, U.K., 1990.

(25) Keith, T.A. *AIMAll,* Version 13.05.06; TK Gristmill Software: Overland Park KS, 2013, http://aim.tkgristmill.com.

(26) (a) Lu, T.; Chen, F. *J. Comput. Chem.* **2012**, *33*, 580. (b) Lu, T.; Chen, F. *J. Mol. Graph. Model.* **2012**, *38*, 314.

(27) Coppens, P. In *Crystallographic Computing;* Ahmed, F. R., Hall, S. R., Huber, C. P., Eds.; Munksgaard: Copenhagen, 1970; p 255.

(28) Altomare, A.; Cascarone, G.; Giacovazzo, C.; Guagliardi, A.; Burla, M. C.; Polidori, G.; Camalli, M. *J. Appl. Crystallogr.* **1994**, *27*, 1045.

(29) Sheldrick, G. M. *SHELXL-97,* A Program for Crystal Structure Refinement; University of Göttingen: Germany, 1997.

(30) Spek, A. L. *Acta Crystalllogr., Sect. A* **1990**, *46*, C34.

DOI: 10.1021/acs.inorgchem.5b00893
Inorg. Chem. 2015, 54, 6010−6019